NUCLEIC ACID THERAPEUTICS
Volume 30, Number 3, 2020

DOI: 10.1089/nat.2019.0825

High Levels of Apoptosis Are Induced in the Human Colon Cancer HT-29 Cell Line by Co-Administration of Sulforaphane and a Peptide Nucleic Acid Targeting miR-15b-5p

Jessica Gasparello,[1] Laura Gambari,[2] Chiara Papi,[1] Andrea Rozzi,[3] Alex Manicardi,[3,*] Roberto Corradini,[3] Roberto Gambari,[1] and Alessia Finotti[1]

Sulforaphane (SFN) is one of most important dietary constituents of broccoli (*Brassica oleracea*) and other cruciferous vegetables, which have been reported to exhibit health benefits, including prevention and therapy of cancer, such as colorectal carcinoma (CRC). The objective of this study was to determine whether the anticancer effect of SFN on colon cancer HT-29 cell line could be improved by the combined treatment with molecules inhibiting microRNAs (miRNAs) involved in CRC. As miRNA inhibiting molecules we focused on peptide-nucleic acids (PNAs). As miRNA to be targeted, miR-15b-5p was selected on the basis of several information present in the literature and confirming that miR-15b-5p is overexpressed in colon cancer patients, and that its targeting decreases cell migration and metastasis in colorectal cancer. In this article, we described for the first time the efficacy of targeting miR-15b-5p by using a PNA against miR-15b-5p (R8-PNA-a15b), functionalized with an octoarginine peptide (R8) for maximizing cellular uptake. The miR-15b-5p downregulation in the colon cancer HT-29 cell line was associated with inhibition of *in vitro* cell growth and activation of the proapoptotic pathway, demonstrated by a sharp increase of late apoptotic cells in HT-29-treated cell populations. A second conclusion of this study is that the R8-PNA-a15b might be proposed in ''combo-therapy'' associated with SFN. To our knowledge, no report is available in the literature on a combination between SFN and miRNA-targeting molecules. Our data demonstrate that this combined treatment leads to a very high proportion of apoptotic HT-29 cells (over 85%), a value higher than the sum of the values of apoptotic cells obtained after singularly administered regents (either SFN or R8-PNA-a15b).

Keywords: apoptosis, peptide nucleic acids, sulforaphane, colon cancer, microRNAs, miR-15b-5p, miRNA targeting

Introduction

Sulforaphane (SFN) is one of the major biologically active products of broccoli (*Brassica oleracea*) and other cruciferous vegetables. It is an isothiocyanate produced by the hydrolysis of the glucosinolate (GL) glucoraphanin by myrosinase of plants and gastrointestinal microflora. Cruciferous vegetables have been reported to exhibit health benefits, including prevention and therapy of cancer [1–5]. For instance, cruciferous vegetables are effective in significantly altering the risk of colorectal neoplasms [6]. Interestingly, SFN has been demonstrated to retain antitumor effects on several *in vitro* and *in vivo* experimental tumor systems, including colon cancer [7–11]. In particular, SFN has been shown to modulate phase I and phase II enzymes, induce growth arrest and/or apoptosis, (especially by regulation of signaling pathways such as Nrf2-Keap1 and NF-κB), inhibit angiogenesis, and regulate the epigenetic machinery.

The objective of this study was to determine whether a combined treatment of SFN with molecules inhibiting microRNAs (miRNAs) might be proposed for increasing the SFN proapoptotic effects. In this respect, it should be underlined that (1) miRNAs are deeply involved in cancer, behaving as both ''oncomiRNAs'' and ''tumor suppressor

[1]Department of Life Sciences and Biotechnology, University of Ferrara, Ferrara, Italy.
[2]Laboratorio RAMSES, IRCCS Istituto Ortopedico Rizzoli, Bologna, Italy.
[3]Department of Chemistry, Life Sciences and Environmental Sustainability, University of Parma, Parma, Italy.
*Current affiliation: Organic and Biomimetic Chemistry Research Group, Department of Organic and Macromolecular Chemistry, Ghent University, Gent, Belgium.

miRNAs'' [12–18]; (2) synergistic effects between anticancer molecules and antagomiRNA molecules targeting oncomiRNA have been reported by different groups [19–21]; (3) among antagomiRNA molecules, peptide nucleic acids (PNAs) have been recently proposed as very useful reagents [22–28].

In this study, we have employed a PNA targeting miR-15b-5p, R8-PNA-a15b, functionalized with an octoarginine peptide (R8) for maximizing cellular uptake, as elsewhere reported [22,23]. The reason in selecting miR-15b as PNA-based targeting was based on the following observations: (1) miR-15b-5p is overexpressed in colon cancer patients [29–31], (2) miR-15b-5p targeting decreases cell migration and metastasis in colorectal cancer [32], and (3) SIRT1 suppresses colorectal cancer metastasis by transcriptional repression of miR-15b-5p [33].

The oncogenic role of miR-15b-5p has been confirmed also in other tumor types, including hepatocellular carcinoma [34], prostate cancer [35], and bladder cancer [36].

As far as anti-miRNA molecules, PNAs are DNA analogues in which the sugar-phosphate backbone has been replaced by N-(2-aminoethyl)-glycine units [37–42]. These very interesting molecules have been described for the first time by Nielsen *et al.* [37] and, despite a radical structural change with respect to DNA and RNA, they are capable of sequence-specific and efficient hybridization with complementary DNA and RNA, forming Watson-Crick double helices [37]. In addition, they are able to generate triple helix formation with double-stranded DNA and perform strand invasion [38–41]. Accordingly, they have been used as very efficient tools for pharmacologic alteration of gene expression, both *in vitro* and *in vivo* [38,39,43,44].

Materials and Methods

Materials

All chemicals and reagents were of analytical grade. SFN (D,L-sulforaphane, 574215-25MG; Merck Millipore, Burlington, MA) was diluted in dimethyl sulfoxide (DMSO) (D8418; Sigma-Aldrich, St. Louis, MO) at final stock concentration of 150 mM. Stock aliquots of SFN were stored at −20°C, protected from the light, and diluted 1:10, at moment of use, in DMSO. All reactants and solvents for PNA synthesis were of analytical grade. Rink amide ChemMatrix®, Fmoc-glycine, acetic anhydride, and m-cresol were obtained from Sigma (St. Louis, MO). Piperidine, *N,N*-Diisopropylethylamine (DIPEA), and trifluoroacetic acid (TFA) were from Alfa Aesar (Haverhill, MA). *N,N,N′,N′*-Tetramethyl-O-(1H-benzotriazol-1-yl)uronium hexafluorophosphate (HBTU) was purchased from TCI Europe (Eschborn, Germany). *N,N*-Dimethylformamide (DMF) was from Scharlab (Barcelona, Spain). Fmoc-protected PNA monomers were purchased from LGC Link (Bellshill, Scotland).

Synthesis and characterization of PNAs

The synthesis and characterization of the R8-PNA-a15b was performed as previously reported for other anti-miRNA PNAs [23]. Briefly, the R8-PNA-a15b was synthesized with an automatic synthesizer Syro I following an Fmoc protocol on a glycine-preloaded resin (Fmoc-Gly-Rink amide ChemMatrix® resin). Each cycle of synthesis was composed by three steps: deprotection of the N-terminal protective group Fmoc (piperidine 20% in DMF, 8 min, twice), coupling of the next commercial monomer (three equivalents of the monomer and the activator HBTU, six equivalents of the non-nucleophilic base DIPEA, and dry DMF, 40 min, twice), and capping of possible unreacted free amine (dry DMF, acetic anhydride, and DIPEA, 89:5:6, 1 min, twice). After the completion of the sequence, the ending Fmoc group was deprotected and the PNA cleaved from the resin using an appropriate cocktail (TFA, m-cresol 9:1, 1 h, twice). The PNA was precipitated in diethyl ether; the precipitate was redessolved in water and purified in reverse-phase high performance liquid chromatography (HPLC) using the following conditions: column Phenomenex Jupiter RPC18, (5 μm, 300 Å, 250×10 mm) 250- 4.6 mm, and 1.7 μM; $T = 40°C$, eluents: A (0.1% TFA in water) and B (0.1% TFA in acetonitrile). Solvent program: flow rate: 4 mL/min; 100% A for five min, then gradient 0%–40% B in 23 min, and 23%–100% B in 3 min. Finally, the identity of the PNA was checked with UPLC-ESI system (see Supplementary Figs. S1–S4) and the quantification was performed using the following ε (260 nm) for the nucleobases: adenine 13,700 M^{-1} cm^{-1}, cytosine 6,600 M^{-1} cm^{-1}, guanine 11,700 M^{-1} cm^{-1}, and thymine 8,600 M^{-1} cm^{-1}.

R8-PNA-a15b. H-R8-TGT AAA CCA TGA TGT GCT-Gly-NH_2; yield = 6.13% UPLC/ESI-MS $R_t = 3.12$ min, molecular weight (MW) calc. = 6,216 g/mol; m/z found (calculated): 1,244.5 (1,244.3) $[MH_5]^{5+}$, 1,037.0 (1,037.1) $[MH_6]^{6+}$, 889.1 (889.0) $[MH_7]^{7+}$, 778.1 (778.0) $[MH_8]^{8+}$, 691.7 (691.7) $[MH_9]^{9+}$, 622.7 (622.6) $[MH_{10}]^{10+}$ (see Supplementary Figs. S1 and S2 for characterization).

R8-PNA-a21. H-R8-TCA ACA TCA GTC TGA TAA-Gly-NH2; yield = 22% UPLC/ESI-MS $R_t = 3.47$ min, MW calc. = 6,169.33 g/mol, m/z found (calculated): 1,234.88 (1,234.87) $[MH_5]^{5+}$, 1,029.24 (1,029.22) $[MH_6]^{6+}$, 882.48 (882.33) $[MH_7]^{7+}$, 772.23 (772.16) $[MH_8]^{8+}$, 686.57 (686.48) $[MH_9]^{9+}$, 618.05 (617.93) $[MH_{10}]^{10+}$ (see Supplementary Figs. S3 and S4 for characterization).

Cell culture conditions

The HT-29 cell line [45,46] was cultured in humidified atmosphere of 5% CO_2/air in RPMI 1640 medium with L-glutamine (EuroClone, Pero, Milano, Italy) supplemented with 10% fetal bovine serum (Biowest, Nuaillé, France), 100 U/mL penicillin, and 100 μg/mL streptomycin (Pen-Strep; Sigma-Aldrich). To verify the effect on proliferation, cell growth was monitored by determining the cell number/mL using a Z2 Coulter Counter (Coulter Electronics, Hialeah, FL).

RNA extraction

Cultured cells were trypsinized (0.05% trypsin and 0.02% EDTA; Sigma-Aldrich) and collected by centrifugation at 1,500 rpm for 8 min at 4°C, washed twice with Dulbecco's phosphate buffered saline (DPBS) 1× (Gibco, Thermo Fischer Scientific, Waltham, MA), and lysed with Tri-Reagent (Sigma-Aldrich), according to manufacturer's instructions. The isolated RNA was washed once with cold 75% ethanol, dried, and dissolved in nuclease-free pure water before use. Obtained RNA was stored at −80°C until use.

Quantitative analyses of miRNAs

MiRNA quantification was performed using real-time reverse transcriptase– quantitative polymerase chain reaction (RT-qPCR) and miRNA-specific primers and probes (reported in Table 1) obtained from Applied Biosystems. RT reactions were performed using TaqMan MicroRNA Reverse Transcription Kit (Applied Biosystems; Thermo Fischer Scientific, Waltham, MA) according to the manufacturer's protocol. All RT reactions, including no-template controls and RT-minus controls, were run in duplicate using TaqMan Universal PCR Master Mix, no AmpErase UNG 2×(Applied Biosystems, Thermo Fischer Scientific), and the CFX96 Touch Real-Time PCR Detection System (BioRad, Hercules, CA). The following amplification program was employed: 95°C for 10 min and 95°C for 15 s, followed by a step at 60°C for 1 min. The last two steps were repeated for 50 cycles, and at the end of each cycle, fluorescence was measured. Data were collected and analyzed using Bio-Rad CFX Manager Software (Bio-Rad). The relative expression was calculated using the comparative cycle threshold method and as reference, snRNA U6 and hsa-let-7c were used to normalize all RNA samples, as previously reported [22,23].

Analysis of apoptosis-related genes

The expression of some genes involved in apoptotic pathway was assessed by RT-qPCR. Three hundred nanograms of total RNA was reverse transcribed by using random hexamers and TaqMan Reverse Transcription PCR Kit (Thermo Fischer Scientific, Waltham, MA) in a final volume of 50 μL. qPCR assays were carried out using gene-specific fluorescently labeled probes. Master Mix 2× and the assays used to quantify caspase-3 (Assay ID: Hs.PT56a.24277143), p53 (Assay ID: Hs.PT.58.123122) and BAK1 (Assay ID: Hs.PT.56a.40435467) mRNA sequences were purchased from IDT (Integrated DNA Technologies, Coralville, IA). The relative mRNA expression was calculated using the comparative cycle threshold method and fold change was calculated as $2^{-\Delta\Delta CT}$. All data were normalized for their starting cDNA content using as reference human RPL13A (Assay ID: Hs04194366_g1; Thermo Fischer Scientific). Duplicate negative controls (no template control) were run in PCR plate to verify specificity and to rule out contamination. All RT-qPCRs were performed in duplicate for both target and normalizer genes [22,23].

Analysis of apoptosis

Apoptosis assays on HT-29 cells were performed with Muse Cell Analyzer instrument (Millipore Corporation, Billerica, MA), and its relative assays according to the instructions supplied by the manufacturer. Muse Annexin V & Dead Cell Kit utilizes annexin V to detect phosphatidyl serine on the external membrane of apoptotic cells. A fluorescent DNA intercalator 7-aminoactinomycin D (7-ADD) is also used as an indicator of cell membrane integrity. 7-ADD is excluded from live, healthy cells, as well as early apoptotic cells, while is able to bind DNA in late apoptosis and dead cells. Four populations of cells can be distinguished in this assay: cells negative to both reagents (live cells), cells positive to annexin V, but negative to 7-AAD (early apoptotic cells), cells negative to annexin V and positive to 7-ADD (cellular debris), and cells positive to both reagents (late apoptotic cells). Cells were washed with sterile Dulbecco's phosphate buffered saline (DPBS) 1×, trypsinized, suspended, and diluted (1:2) with the Muse Annexin V & Dead Cell reagent. Samples were gently mixed and incubated at room temperature, protected from the light for 15 min. Samples were analyzed using Muse Cell Analyzer and data from prepared samples were acquired and recorded utilizing the Annexin V and Dead Cell Software Module (Millipore) [23], while the apoptotic status, based on caspase-3/7 activation, was detected using The Muse Caspase-3/7 Kit. The assay is based on the use of a DNA binding dye, linked to a DEVD peptide substrate. When bound to DEVD, the dye is unable to bind DNA, while the cleavage by active caspase-3/7 in the cell results in release of the dye that translocates to the nucleus and binds the DNA, increasing the fluorescence. As for Annexin V assay, in this case, 7-ADD as indicator of cell membrane integrity was employed. Briefly, cells were detached, washed with DPBS 1×, and 50 μL of cell suspension cells was incubated with 5 μL of caspase-3/7 working solution (obtained from 1:8 dilution of Muse Caspase-3/7 Reagent with 1×PBS). After an incubation of 30 min at 37°C, 150 μL of 7-AAD working solution (obtained from 1:75 dilution of 7-ADD in 1×Assay Buffer BA) was added, and the mixture was incubated for 5 min at room temperature, protected from the light. Samples were analyzed using Muse Cell Analyzer instrument and Caspase-3/7 software.

Table 1. List of Assays Employed for miRNA Detection

miRNA name	*Assay ID*
hsa-miR-15b-5p	000390
hsa-miR-221-3p	000524
hsa-miR-222-3p	002276
hsa-miR-21-5p	000397
hsa-snRNA U6	001973
hsa-let-7c-5p	000379

Combination analysis of treatment with SFN and PNA-a15b

The drug combination analysis was performed using the method developed by Chou and Talalay [47–49]. The calculations of combination index (CI) were generated using CompuSyn (www.combosyn.com), a freely available web-based tool for drug synergy analysis based on the Chou–Talalay method [50–53]. The Compusyn software defines synergic interactions between the drugs when CI value is <1, and values of CI lower that 0.5 are indicative of clear synergic effects obtained by drug combination. On the contrary, CI values close to 1 are indicative of additive effect and values >1 indicate antagonism.

Statistics

Results are expressed as mean ± standard error of the mean. Comparisons between groups were made by using paired Student's *t*-test. Statistical significance was defined as significant ($^*P < 0.05$) or highly significant ($^{**}P < 0.01$ and $^{***}P < 0.001$).

Results

SFN mediated induction of apoptosis of colon cancer HT-29 cells

When HT-29 cells were cultured in the presence of increasing concentrations of SFN (7.5, 15, 30 and 60 μM) for 3

days, cell growth was inhibited and this effect was found associated with an increase of apoptosis. Figure 1A shows that increasing the concentration of SFN causes inhibition of cell growth of HT-29 cells.

Figure 1B and C show the effects of SFN on apoptosis of HT-29 cells cultured in the presence of SFN and analyzed employing the Annexin V assay. In Fig. 1B, the results from a representative experiment are shown, while in Fig. 1C, a summary of the data gathered from three independent experiments is presented. The vehicle for SFN (DMSO) exhibited no proapoptotic effects. The experiment shown in Fig. 1D further confirms the proapoptotic effects of SFN on HT-29 cells. In this experiment, caspase-3 mRNA was quantified by RT-qPCR. The obtained results demonstrate a sharp and significant increase of caspase-3 mRNA in HT-29 cells treated with 30 and 60 μM SFN, respectively ($P < 0.05$). Altogether, the results presented in Fig. 1 demonstrate that SFN is a strong inhibitor of cell growth of HT-29 cells (Fig. 1A) and that this effect is associated with the induction of apoptosis (Fig. 1B–D).

Targeting miR-15b-5p with the R8-PNA-a15b molecule downregulated miR-15b-5p and induces inhibition of HT-29 cell growth associated with proapoptotic effects

In consideration of the involvement of miR-15b-5p on colon cancer, we have designed and tested a PNA molecule (R8-PNA-a15b) targeting miR-15b-5p and functionalized with an octoarginine peptide (R8) for maximizing intracellular uptake, as recently reported by our group [23]. No effects of the R8 peptide on cell growth and apoptosis were detected, fully in agreement with observations reported elsewhere by our and other research groups [22,23,54]. The results obtained using the PNA-a15b are shown in Fig. 2 and demonstrate that the treatment of HT-29 cells with the R8-PNA-a15b reduced miR-15b-5p-specific hybridization (Fig. 2A), induced apoptosis (Fig. 2B, C), and inhibited HT-29 cell growth (Fig. 2D, E). With respect to miR-15b-5p-specific inhibition (Fig. 2A), while inhibitory effects by PNA-a15b were reproducibly observed on miR-15b-5p, no inhibitory activity was found on miR-221-3p, miR-222-3p, and miR-425-3p and only a low effect was observed on miR-21-5p (Fig. 2A, left side of the panel). Conversely, PNA-a21 was found to inhibit miR-21-5p, but is fully inactive on miR-15b-5p. These results support the conclusion that the effects of PNA-a15b are specific; the partial inhibition of miR-21-5p by PNA-a15b is among expected effects of PNA-based treatments, considering that anti-miRNA PNAs might lead, in addition to inhibition of the specific miRNA targets, to inhibition of other miRNAs ($\sim$7%–10% of the miRNome is altered by miRNA targeting PNAs, accordingly with data based on next-generation sequencing) [55]. These novel data (to our knowledge, no study is available on the effects of PNA against miR-15b-5p) support the concept that inhibition of miR-15b-5p in colon cancer cells is associated with antitumor activity *in vitro*.

Co-treatment of HT-29 cells with R8-PNA-a15b and SFN: effects on apoptosis

When the HT-29 cell line was cultured in the presence of singularly administered R8-PNA-a15b or SFN and the data obtained were compared with HT-29 cell treated with a combination of R8-PNA-a15b and SFN, the induction of apoptosis in the combined treatment was significantly higher. In this set of experiments, PNA was used at 8 μM and SFN at 30 μM. The treatments were carried out for 3 days. As far as the effects on apoptosis, Fig. 3A shows representative results obtained with Annexin V assay, while Fig. 3B reports a summary of the data obtained in three independent experiments. The remarkable high induction of apoptosis in the combined treatment was fully confirmed by performing a caspase-3/7 assay shown in Fig. 4 (a representative experiment in Fig. 4A and a summary of the data obtained in Fig. 4B). In particular, we found that the ''late apoptotic cells'' in the combined treatment are higher than the sum of the single treatments.

To further verify whether SFN and PNA-a15b synergistically induced apoptosis of HT-29 colon cancer cells, we employed suboptimal concentrations of SFN (20 μM) and PNA-a15b (6 μM). HT-29 cells were cultured for 3 days with 20 μM SFN in the presence of increasing concentrations of PNA-a15b (2, 4, 6, and 8 μM) (Fig. 5B). In parallel, HT-29 cells were treated for the same length of time with 6 μM PNA-a15b in the presence of increasing concentrations of SFN (10, 20, 30, and 40 μM) (Fig. 5D). We first demonstrated that apoptosis-associated genes (caspase-3, p53, and BAK1) [56–58] were activated even at these low concentrations of SFN and PNA-a15b (Fig. 5A, C). The results of the effects of combined treatments are shown in Fig. 5B, D, and E–G, clearly indicating that in most of the drug combinations performed using the highest suboptimal doses of SFN and PNA-a15b, apoptosis induction was obtained at levels higher than those predicted performing the sum of the % apoptosis obtained, considering the levels relative to singularly administered SFN and PNA-a15b (compare Fig. 5E and F). By exploring pharmacological additivity performing isobologram analysis and calculating the CI according to Chou and Talalay [47–49] using the CompuSyn software [50], we obtained strong evidences of synergism (CI <1), as depicted in Fig. 5G.

Co-treatment of HT-29 cells with R8-PNA-a15b and SFN: increase of inhibitory effects on cell growth

When HT-29 cells were cultured in the presence of a combination of R8-PNA-a15b and SFN, the inhibition of cell growth in the combined treatment was higher than when R8-PNA-a15b or SFN was administered singularly. This conclusion is supported by the data shown in Fig. 6A and B. As expected, inhibition of miR-15b-5p hybridization was found only when RNA was extracted from R8-PNA-a15b-treated cells (either administered singularly or in combination with SFN) (Fig. 6C).

Discussion

Colon cancer (CRC) patients express at high levels miR-15b-5p, promoting malignant progression. The involvement of miR-15b-5p in colon cancer is sustained by the study by Li *et al.* [32], who reported that inhibition of miR-15b activity by adenovirus carrying antimiR-15b sequence significantly increases expression of metastasis suppressor 1 and decreases colony formation ability, invasion, and migration of HCT116 cells *in vitro* and liver metastasis of HCT116 tumors *in vivo*.

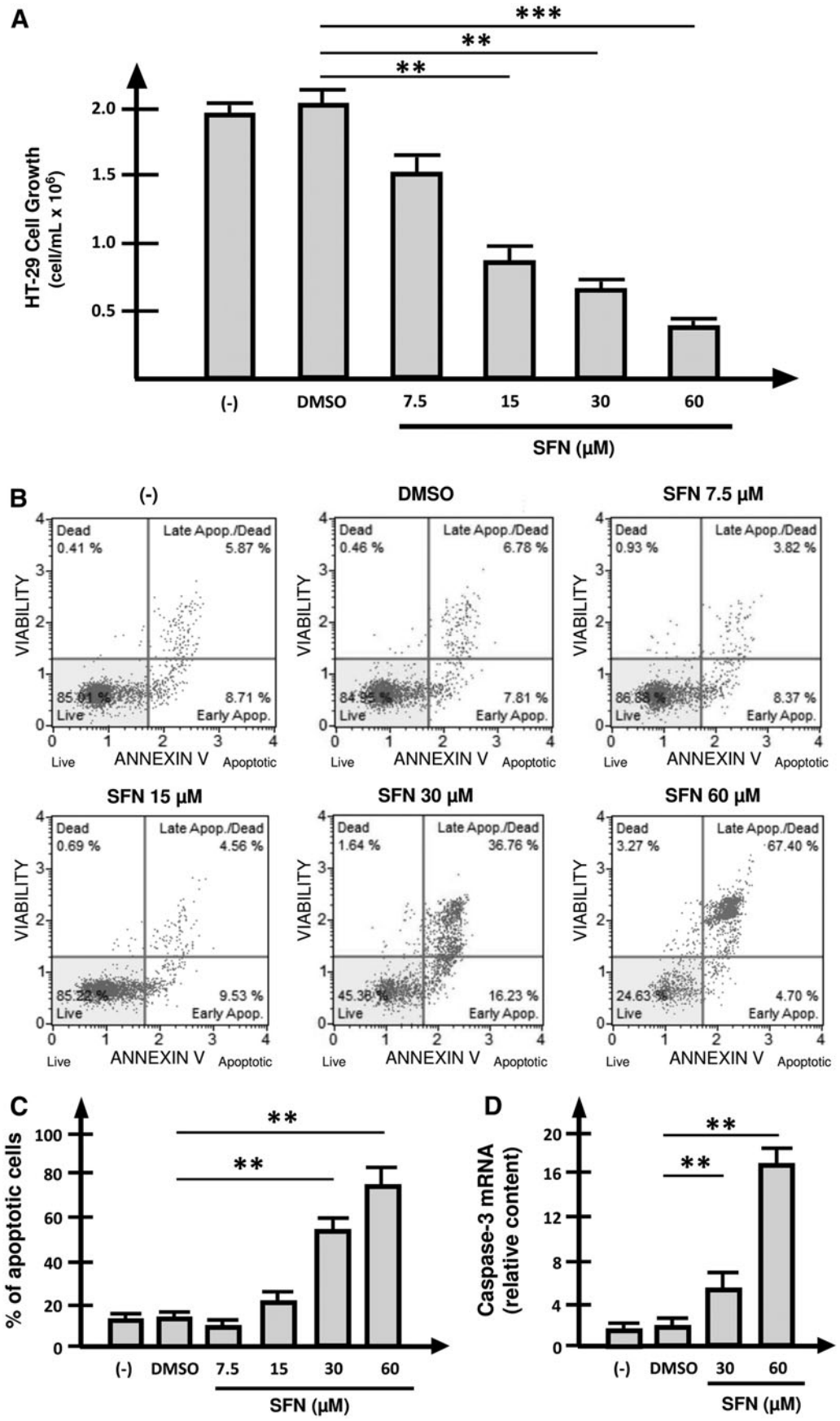

FIG. 1. Effects on HT-29 colon cancer cells of increasing concentrations of SFN on cell growth **(A)**, apoptosis **(B, C),** and caspase-3 mRNA production **(D)**. Analyses were performed after 3 days of exposure to SFN. $^{**}P<0.01$; $^{***}P<0.001$. SFN, sulforaphane.

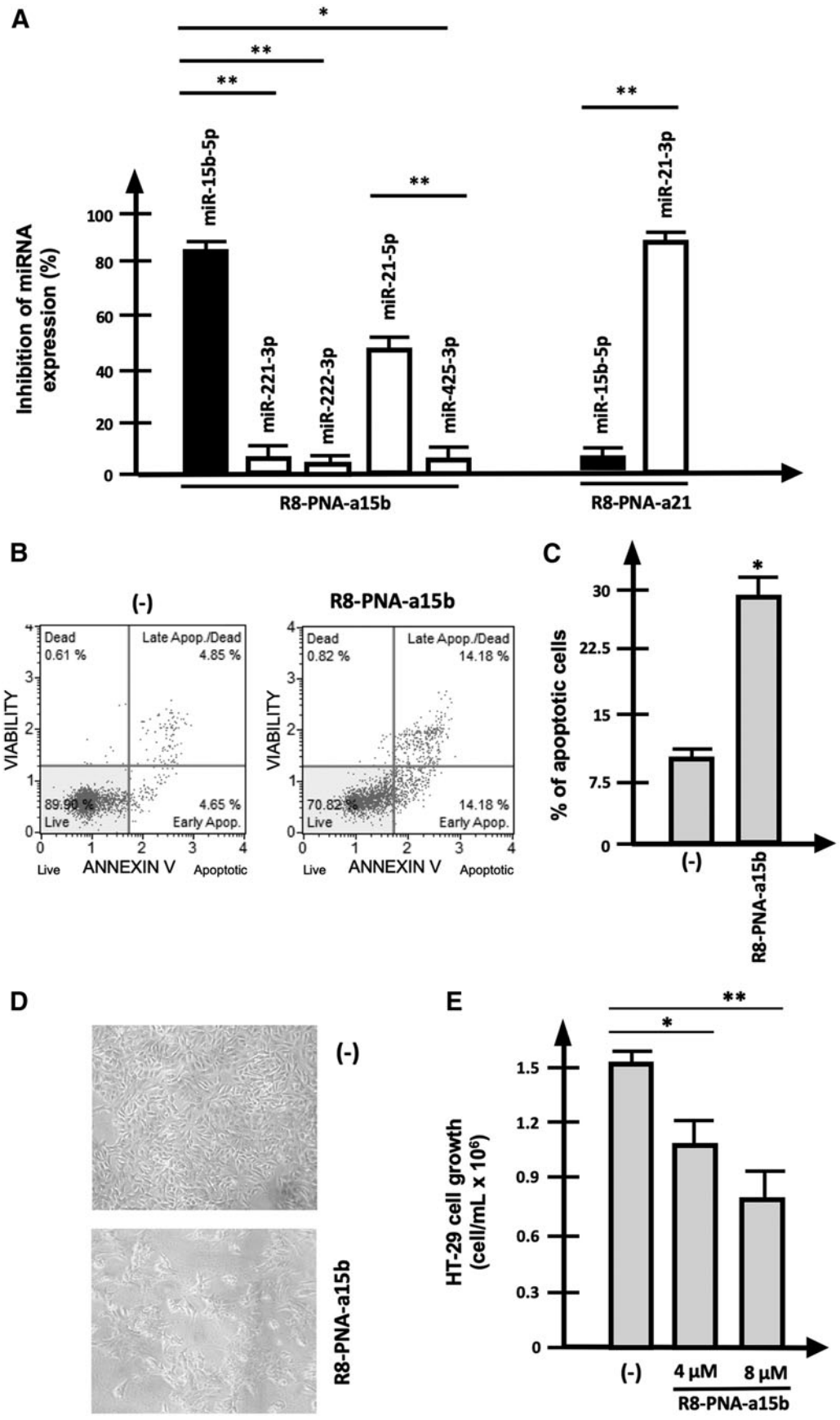

FIG. 2. Effects of the R8-PNA-a15b on HT-29 colon cancer cells. **(A)** Effects on RT-qPCR amplification of miR-15b-5p; **(B, C)** effects of PNA-a15b on apoptosis; **(D, E)** effects on cell growth. Analyses were performed after 3 days of exposure to the R8-PNA-a15b. $*P < 0.05$; $**P < 0.01$. PNA, peptide nucleic acid; RT-qPCR, reverse transcriptase–quantitative polymerase chain reaction.

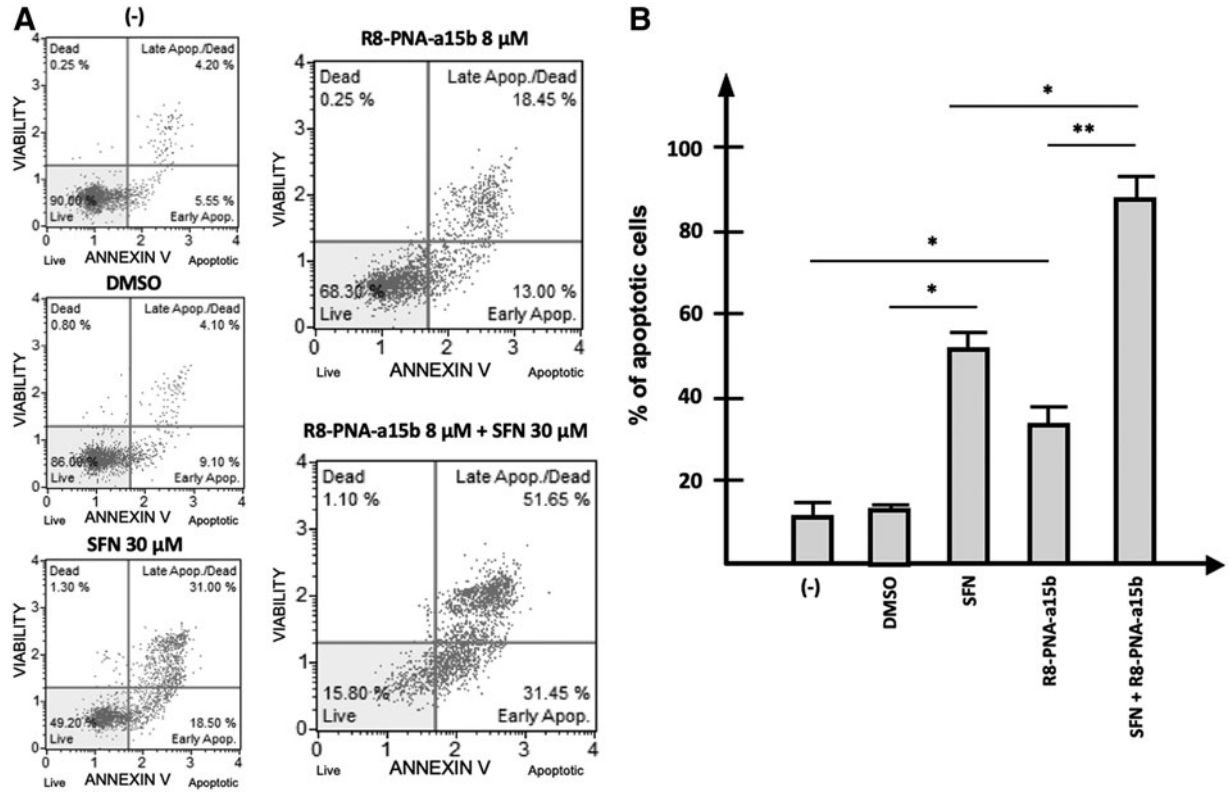

FIG. 3. Effects of a combined treatment with the R8-PNA-a15b and SFN on apoptosis analyzed by the Annexin V assay **(A, B)**. HT-29 colon cancer cells were untreated, or treated for 3 days with the SFN vehicle DMSO, with 30 µM SFN, with 8 µM R8-PNA-a15b, or with both with 30 µM SFN and 8 µM R8-PNA-a15b. $*P<0.05$; $**P<0.01$. DMSO, dimethyl sulfoxide.

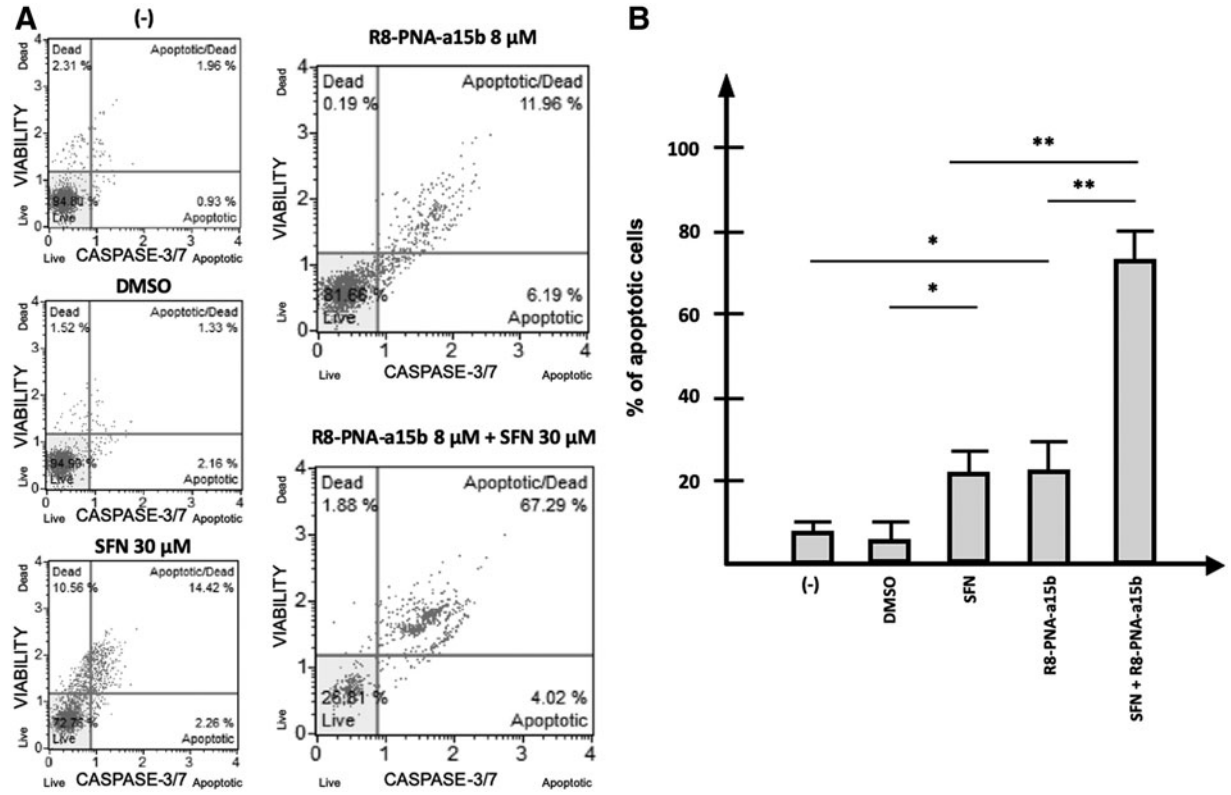

FIG. 4. Effects of a combined treatment with the R8-PNA-a15b and SFN on apoptosis analyzed by the caspase-3/7 assay **(A, B)**. HT-29 colon cancer cells were untreated, or treated for 3 days with the SFN vehicle DMSO, with 30 µM SFN, with 8 µM R8-PNA-a15b, or with both 30 µM SFN and 8 µM R8-PNA-a15b. $*P<0.05$; $**P<0.01$.

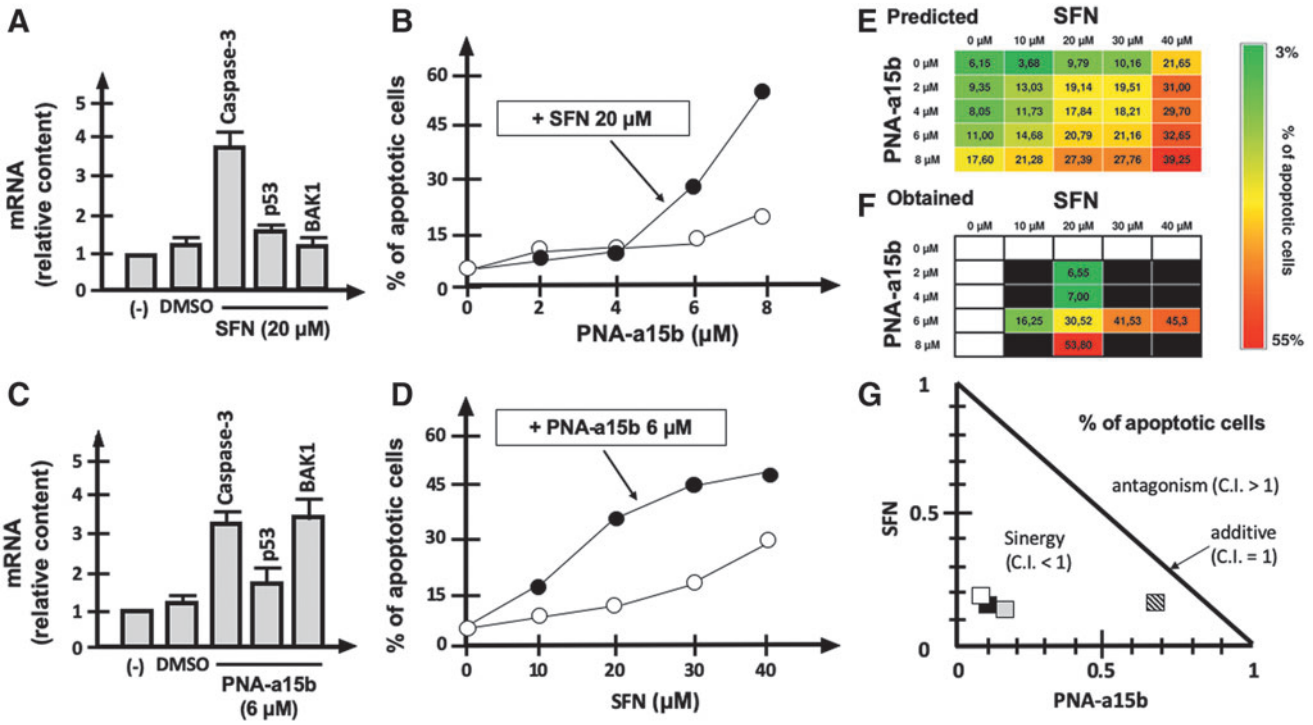

FIG. 5. Evaluation of possible synergic effects between SFN and PNA-a15b. **(A, C)** Effects of singularly administrated SFN and PNA-a15b (respectively, at 20 and 6 μM) on caspase-3, p53, and BAK1 mRNAs, studied by RT-qPCR. **(B, D)** Effects of incremental concentrations of PNA-a15b **(B)** or SFN **(D)** on percentage of apoptotic cells. In **(B),** the concentration of SFN (20 μM) was maintained standard, while incremental concentrations (from 2 to 8 μM) of PNA-a15b were employed. On the contrary, in **(D),** the concentration of PNA-a15b (6 μM) was maintained standard, while incremental concentrations (from 10 to 40 μM) of SFN were employed. **(E, F)** Percentage of apoptotic cells is reported, predicted by the sum of singularly administrated drugs **(E)** or effectively obtained during the co-treatment procedures **(F)**, **(G)** isobologram showing the CI according to Chou and Talalay [47–49] method obtained by SFN and PNA-a15b co-treatment. The CompuSyn software was employed [50]. All the reported treatments were carried out for 3 days. CI, combination index.

In another study, Sun *et al.* [33] demonstrated that SIRT1 suppressed CRC metastasis *in vitro* and *in vivo* as a negative regulator for miR-15b-5p transcription. Mechanistically, SIRT1 impaired regulatory effects of activator protein (AP-1) on miR-15b-5p transactivation through deacetylation of AP-1. Accordingly, miR-15b-5p could be considered a target for possible personalized approaches for CRC.

In this article, we described for the first time targeting of miR-15b-5p by using a PNA as anti-miR. This miR-15b-5p downregulation in colon cancer HT-29 cells was associated with inhibition of *in vitro* cell growth and activation of the proapoptotic pathway, demonstrated by a sharp increase of late apoptotic cells in HT-29-treated cell populations.

A second conclusion of our article is that the R8-PNA-a15b might be proposed in ''combo-therapy'' associated with the use of other proapoptotic agents. We focused our interest of SFN, considering the fact that this component of *B. oleracea* extracts is a recognized inducer of apoptosis in several tumor systems, including hepatocellular carcinoma [34], prostate cancer [35], and bladder cancer [36]. To our knowledge, no report is available in the literature on a combination between SFN and miRNA-targeting molecules. Our data demonstrate that this combined treatment leads to a very high proportion of apoptotic HT-29 cells (>85%), a value higher than the sum of the values of apoptotic cells obtained after singularly administered regents (either SFN or the R8-PNA-a15b).

Further studies will clarify the effects of the R8-PNA-a15b on the molecular targets of miR-15b-5p. Moreover, *in vivo* experiments will clarify whether this approach can be proposed for combo-therapy of CRC patients.

In conclusion, our results support the concept that anti-miR strategy could lead to therapeutic relevant inhibition of miRNA-dependent effects and that PNA-based anti-miRNA molecules are very promising reagents to regulate tumor cell growth; further research on PNA analogues to increase efficiency of delivery, stability, and control of intracellular distribution for specific targets, that is, mature miRNA, pre-miRNA, or pri-miRNA, are further steps for the selection of best candidate drugs. Finally, our study strongly indicates that the combined treatment of target cells with miRNA targeting PNAs (in this study, a PNA targeting miR-15b-5p) and antitumor agents (in this study SFN) is a promising strategy to increase efficacy and limit, at least in theory, side effects.

Regarding the use of dietary constituents to promote anticancer effects, particularly GLs-isothiocyanates (ITCs), it is important to note that the efficiency of conversion of GLs to ITCs is a key factor in controlling their health-promoting properties and is exerted by active myrosinase. Interestingly,

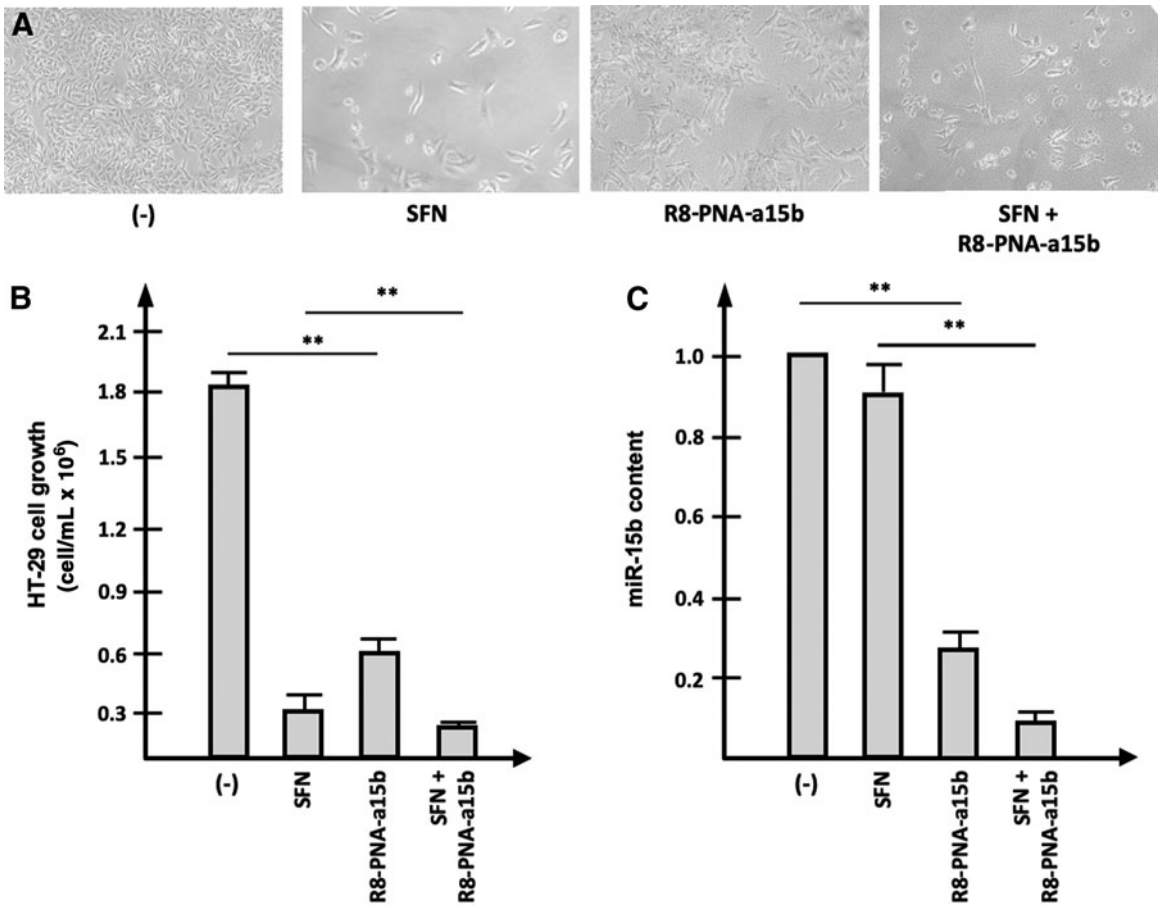

FIG. 6. Effects of a combined treatment with the R8-PNA-a15b and SFN on HT-29 cell morphology **(A)** and cell growth **(B)**. In **(C),** the effects on miR-15b-5p amplification are presented. The treatment was carried out for 3 days. $^{**}P < 0.01$.

cooking of raw vegetables inactivates plant myrosinases, limiting ITC production. Furthermore, the gastrointestinal microflora can convert GLs to ITCs and thus acts as a significant factor for the health-promoting benefits associated with the consumption of cruciferous vegetables. Notably, changes in the gut microbiota occur in CRC patients and could impair ITC production. This work highlighted the important antiapoptotic effect of SFN and combination of SFN and R8-PNA-a15b, thus suggesting how a local therapy, besides oral consumption of SFN precursors, with these agents could be beneficial toward these patients.

Acknowledgment

We thank Federica Fontana for her technical assistance.

Author Disclosure Statement

No competing financial interests exist.

Funding Information

This work has benefited from the equipment and framework of the COMP-HUB Initiative, funded by the ''Departments of Excellence'' program of the Italian Ministry for Education, University and Research (MIUR, 2018-2022). This work was granted by CIB, by FAR, and by AIRC (IG 13575: peptide nucleic acids targeting oncomiR and tumor-suppressor miRNAs: cancer diagnosis and therapy).

Supplementary Material

Supplementary Figure S1
Supplementary Figure S2
Supplementary Figure S3
Supplementary Figure S4

References

1. Conzatti A, FC Fróes, ID Schweigert Perry and CG Souza. (2014). Clinical and molecular evidence of the consumption of broccoli, glucoraphanin and sulforaphane in humans. Nutr Hosp 31:559–569.
2. Latté KP, KE Appel and A Lampen. (2011). Health benefits and possible risks of broccoli—an overview. Food Chem Toxicol 49:3287–3309.
3. Bachiega P, JM Salgado, JE de Carvalho, ALTG Ruiz, K Schwarz, T Tezotto and MC Morzelle. (2016). Antioxidant and antiproliferative activities in different maturation stages of broccoli (*Brassica oleracea* Italica) biofortified with selenium. Food Chem 190:771–776.
4. Sturm C and AE Wagner. (2017). Brassica-derived plant bioactives as modulators of chemopreventive and inflammatory signaling pathways. Int J Mol Sci 18:E1890.

5. Herr I and MW Büchler. (2010). Dietary constituents of broccoli and other cruciferous vegetables: implications for prevention and therapy of cancer. Cancer Treat Rev 36: 377–383.
6. Tse G and GD Eslick. (2014). Cruciferous vegetables and risk of colorectal neoplasms: a systematic review and meta-analysis. Nutr Cancer 66:128–139.
7. Langner E, MK Lemieszek and W Rzeski. (2019). Lycopene, sulforaphane, quercetin, and curcumin applied together show improved antiproliferative potential in colon cancer cells in vitro. J Food Biochem 43:e12802.
8. Tafakh MS, M Saidijam, T Ranjbarnejad, S Malih, S Mirzamohammadi and R Najafi. (2018). Sulforaphane, a chemopreventive compound, inhibits cyclooxygenase-2 and microsomal prostaglandin e synthase-1 expression in human HT-29 colon cancer cells. Cells Tissues Organs 206: 46–53.
9. Bessler H and M Djaldetti. (2018). Broccoli and human health: immunomodulatory effect of sulforaphane in a model of colon cancer. Int J Food Sci Nutr 69:946–953.
10. Martin SL, R Kala and TO Tollefsbol. (2018). Mechanisms for the inhibition of colon cancer cells by sulforaphane through epigenetic modulation of microRNA-21 and human telomerase reverse transcriptase (hTERT) down-regulation. Curr Cancer Drug Targets 18:97–106.
11. Liu KC, TY Shih, CL Kuo, YS Ma, JL Yang, PP Wu, YP Huang, KC Lai and JG Chung. (2016). Sulforaphane induces cell death through G2/M phase arrest and triggers apoptosis in HCT 116 human colon cancer cells. Am J Chin Med 44:1289–1310.
12. Fabbri M, M Ivan, A Cimmino, M Negrini and GA Calin. (2007). Regulatory mechanisms of microRNAs involvement in cancer. Expert Opin Biol Ther 7:1009–1019.
13. Anvarnia A, F Mohaddes-Gharamaleki, M Asadi, M Akbari, B Yousefi and D Shanehbandi. (2019). Dysregulated microRNAs in colorectal carcinogenesis: new insight to cell survival and apoptosis regulation. J Cell Physiol 234: 21683–21693.
14. Soleimani A, F Rahmani, GA Ferns, M Ryzhikov, A Avan and SM Hassanian. (2018). Role of regulatory oncogenic or tumor suppressor miRNAs of PI3K/AKT signaling axis in the pathogenesis of colorectal cancer. Curr Pharm Des 24: 4605–4610.
15. Asadzadeh Z, B Mansoori, A Mohammadi, M Aghajani, K Haji-Asgarzadeh, E Safarzadeh, A Mokhtarzadeh, PHG Duijf and B Baradaran. (2018). microRNAs in cancer stem cells: biology, pathways, and therapeutic opportunities. J Cell Physiol 234:10002–10017.
16. Mollaei H, R Safaralizadeh and Z Rostami. (2019). MicroRNA replacement therapy in cancer. J Cell Physiol 234: 12369–12384.
17. Zhang L, Y Liao and L Tang. (2019). MicroRNA-34 family: a potential tumor suppressor and therapeutic candidate in cancer. J Exp Clin Cancer Res 38:53.
18. Gambari R, E Brognara, DA Spandidos and E Fabbri. (2016). Targeting oncomiRNAs and mimicking tumor suppressor miRNAs: new trends in the development of miRNA therapeutic strategies in oncology (review). Int J Oncol 49:5–32.
19. Zhang L, L He, H Zhang and Y Chen. (2018). Knockdown of MiR-20a enhances sensitivity of colorectal cancer cells to cisplatin by increasing ASK1 expression. Cell Physiol Biochem 47:1432–1441.
20. Bertucci A, EA Prasetyanto, D Septiadi, A Manicardi, E Brognara, R Gambari, R Corradini and L De Cola. (2015). Combined delivery of temozolomide and anti-miR221 PNA using mesoporous silica nanoparticles induces apoptosis in resistant glioma cells. Small 11:5687–5695.
21. Miroshnichenko S and O Patutina. (2019). Enhanced inhibition of tumorigenesis using combinations of miRNA-targeted therapeutics. Front Pharmacol 10:488.
22. Fabbri E, A Manicardi, T Tedeschi, S Sforza, N Bianchi, E Brognara, A Finotti, G Breveglieri, M Borgatti, et al. (2011). Modulation of the biological activity of microRNA-210 with peptide nucleic acids (PNAs). ChemMedChem 6: 2192–2202.
23. Brognara E, E Fabbri, E Bazzoli, G Montagner, C Ghimenton, A Eccher, C Cantù, A Manicardi, N Bianchi, et al. (2014). Uptake by human glioma cell lines and biological effects of a peptide-nucleic acids targeting miR-221. J Neurooncol 118:19–28.
24. Beavers KR, TA Werfel, T Shen, TE Kavanaugh, KV Kilchrist, JW Mares, JS Fain, CB Wiese, KC Vickers, SM Weiss and CL Duvall. (2016). Porous silicon and polymer nanocomposites for delivery of peptide nucleic acids as anti-MicroRNA therapies. Adv Mater 28:7984–7992.
25. Gupta A, E Quijano, Y Liu, R Bahal, SE Scanlon, E Song, WC Hsieh, DE Braddock, DH Ly, WM Saltzman and PM Glazer. (2017). Anti-tumor activity of miniPEG-γ-modified PNAs to inhibit microRNA-210 for cancer therapy. Mol Ther Nucleic Acids 9:111–119.
26. Manicardi A, R Gambari, L de Cola and R Corradini. (2018). Preparation of anti-miR PNAs for drug development and nanomedicine. Methods Mol Biol 1811:49–63.
27. Seo YE, HW Suh, R Bahal, A Josowitz, J Zhang, E Song, J Cui, S Noorbakhsh, C Jackson, et al. (2019). Nanoparticle-mediated intratumoral inhibition of miR-21 for improved survival in glioblastoma. Biomaterials 201:87–98.
28. Milani R, E Brognara, E Fabbri, A Manicardi, R Corradini, A Finotti, J Gasparello, M Borgatti, LC Cosenza, et al. (2019). Targeting miR-155-5p and miR-221-3p by peptide nucleic acids induces caspase-3 activation and apoptosis in temozolomide-resistant T98G glioma cells. Int J Oncol 55: 59–68.
29. Xi Y, A Formentini, M Chien, DB Weir, JJ Russo, J Ju, M Kornmann and J Ju. (2006). Prognostic values of microRNAs in colorectal cancer. Biomark Insights 2:113–121.
30. Yang J, D Ma, A Fesler, H Zhai, A Leamniramit, W Li, S Wu and J Ju. (2016). Expression analysis of microRNA as prognostic biomarkers in colorectal cancer. Oncotarget 8: 52403–52412.
31. Pan C, X Yan, H Li, L Huang, M Yin, Y Yang, R Gao, L Hong, Y Ma, et al. (2017). Systematic literature review and clinical validation of circulating microRNAs as diagnostic biomarkers for colorectal cancer. Oncotarget 8:68317–68328.
32. Li J, Y Chen, X Guo, L Zhou, Z Jia, Y Tang, L Lin, W Liu and C Ren. (2016). Inhibition of miR-15b decreases cell migration and metastasis in colorectal cancer. Tumour Biol 37:8765–8773.
33. Sun LN, Z Zhi, LY Chen, Q Zhou, XM Li, WJ Gan, S Chen, M Yang, Y Liu, et al. (2017). SIRT1 suppresses colorectal cancer metastasis by transcriptional repression of miR-15b-5p. Cancer Lett 409:104–115.
34. Pan WY, JH Zeng, DY Wen, JY Wang, PP Wang, G Chen and ZB Feng. (2019). Oncogenic value of microRNA-15b-5p in hepatocellular carcinoma and a bioinformatics investigation. Oncol Lett 17:1695–1713.
35. Chen R, L Sheng, HJ Zhang, M Ji and WQ Qian. (2018). miR-15b-5p facilitates the tumorigenicity by targeting

RECK and predicts tumour recurrence in prostate cancer. J Cell Mol Med 22:1855–1863.
36. Wang F, Y Zu, S Zhu, Y Yang, W Huang, H Xie and G Li. (2018). Long noncoding RNA MAGI2-AS3 regulates CCDC19 expression by sponging miR-15b-5p and suppresses bladder cancer progression. Biochem Biophys Res Commun 507:231–235.
37. Nielsen PE, M Egholm, RH Berg, and O Buchardt. (1991). Sequence-selective recognition of DNA by strand displacement with a thymine-substituted polyamide. Science 254:1497–1500.
38. Nielsen PE. (2001). Targeting double stranded DNA with peptide nucleic acid (PNA). Curr Med Chem 8:545–550.
39. Borgatti M, I Lampronti, A Romanelli, C Pedone, M Saviano, N Bianchi, C Mischiati and R Gambari. (2003). Transcription factor decoy molecules based on a peptide nucleic acid (PNA)-DNA chimera mimicking Sp1 binding sites. J Biol Chem 278:7500–7509.
40. Gambari R. (2001). Peptide-nucleic acids (PNAs): a tool for the development of gene expression modifiers. Curr Pharm Des 7:1839–1862.
41. Gambari R. (2004). Biological activity and delivery of peptide nucleic acids (PNA)-DNA chimeras for transcription factor decoy (TFD) pharmacotherapy. Curr Med Chem 11:1253–1263.
42. Nielsen PE. (2010). Peptide nucleic acids (PNA) in chemical biology and drug discovery. Chem Biodivers 7:786–804.
43. Nielsen PE. (2010). Gene targeting and expression modulation by peptide nucleic acids (PNA). Curr Pharm Des 16: 3118–3123.
44. Quijano E, R Bahal, A Ricciardi, WM Saltzman and PM Glazer. (2017). Therapeutic peptide nucleic acids: principles, limitations, and opportunities. Yale J Biol Med 90: 583–598.
45. Shirafkan N, N Shomali, T Kazemi, D Shanehbandi, M Ghasabi, E Baghbani, M Ganji, V Khaze, B Mansoori and B Baradaran. (2018). microRNA-193a-5p inhibits migration of human HT-29 colon cancer cells via suppression of metastasis pathway. J Cell Biochem [Epub ahead of print]. DOI: 10.1002/jcb.28164.
46. Gasparello J, M Allegretti, E Tremante, E Fabbri, CA Amoreo, P Romania, E Melucci, K Messana, M Borgatti, et al. (2018). Liquid biopsy in mice bearing colorectal carcinoma xenografts: gateways regulating the levels of circulating tumor DNA (ctDNA) and miRNA (ctmiRNA). J Exp Clin Cancer Res 37:124.
47. Chou TC and P Talalay. (1984). Quantitative analysis of dose-effect relationships: the combined effects of multiple drugs or enzyme inhibitors. Adv Enzym Regul 22:27–55.
48. Chou TC. (2006). Theoretical basis, experimental design, and computerized simulation of synergism and antagonism in drug combination studies. Pharmacol Rev 68:621–681.
49. Chou TC. (2010). Drug combination studies and their synergy quantification using the Chou-Talalay method. Cancer Res 70:440–446.
50. Zhang N, JN Fu, and TC Chou. (2016). Synergistic combination of microtubule targeting anticancer fludelone with cytoprotective panaxytriol derived from panax ginseng against MX-1 cells in vitro: experimental design and data analysis using the combination index method. Am J Cancer Res. 6:97–104.
51. Er JL, PN Goh, CY Lee, YJ Tan, LW Hii, CW Mai, FF Chung and CO Leong. (2018). Identification of inhibitors synergizing gemcitabine sensitivity in the squamous subtype of pancreatic ductal adenocarcinoma (PDAC). Apoptosis 23:343–355.
52. Low SY, BS Tan, HL Choo, KH Tiong, AS Khoo and CO Leong. (2012). Suppression of BCL-2 synergizes cisplatin sensitivity in nasopharyngeal carcinoma cells. Cancer Lett 314:166–175.
53. Wong SW, KH Tiong, WY Kong, YC Yue, CH Chua, JY Lim, CY Lee, SI Quah, C Fow, et al. (2011). Rapamycin synergizes cisplatin sensitivity in basal-like breast cancer cells through upregulation of p73. Breast Cancer Res Treat 128:301–313.
54. Chugh A, F Eudes, and YS Shim. (2010). Cell-penetrating peptides: nanocarrier for macromolecule delivery in living cells. IUBMB Life 62:183–193.
55. Finotti A, J Gasparello, E Fabbri, A Tamanini, R Corradini, MC Dechecchi, G Cabrini and R Gambari. (2019). Enhancing the expression of CFTR using antisense molecules against microRNA miR-145-5p. Am J Respir Crit Care Med 199:1443–1444.
56. Porter AG and RU Jänicke. (1999). Emerging roles of caspase-3 in apoptosis. Cell Death Differ 6:99–104.
57. Aubrey BJ, GL Kelly, A Janic, MJ Herold and A Strasser. (2018). How does p53 induce apoptosis and how does this relate to p53-mediated tumour suppression? Cell Death Differ 25:104–113.
58. Lindqvist LM and DL Vaux. (2014). BCL2 and related prosurvival proteins require BAK1 and BAX to affect autophagy. Autophagy 10:1474–1475

Address correspondence to:
Roberto Gambari, PhD
Department of Life Sciences and Biotechnology
University of Ferrara
Via Fossato di Mortara n.74
Ferrara 44121
Italy

E-mail: gam@unife.it

Received for publication September 17, 2019; accepted after revision December 24, 2019; published online February 17, 2020.